CHARACTERISATION OF A SMALL RING-CUSP GRIDDED ION ENGINE USING ALTERNATIVE PROPELLANTS

GLASGOW, SCOTLAND | 20 – 23 MAY 2024

Nazareno Fazio [(1)], Igor O. Golosnoy [(2)], Stephen B. Gabriel [(3)], Franco Bosi [(4)], and Francesco Guarducci [(5)]

[(1)(2)(3)] University of Southampton, University Road, SO17 1BJ, Southampton, UK
[(1)(4)(5)] Mars Space Ltd, Unit D3, Adanac Drive, SO16 0BT, Southampton, UK
Email: [(1)] nazareno.fazio@mars-space.co.uk
[(2)] I.Golosnoy@soton.ac.uk
[(3)] sbg2@soton.ac.uk
[(4)] franco.bosi@mars-space.co.uk
[(5)] francesco.guarducci@mars-space.co.uk

KEYWORDS: Gridded Ion Engine, Propellants, Xenon, Krypton, Performance Parameters

ABSTRACT:

Xenon is the preferred propellant for electric propulsion thrusters, providing high thruster efficiency and long life. However, xenon is extremely expensive and has limited availability, which could impose serious constraints on the use of electric propulsion in some future missions. This report presents the results of the experimental characterization of a small ring-cusp discharge chamber using xenon (as baseline), krypton and a 1:4 Xe/Kr mixture.

These results represent the worst-case scenario for alternative propellants, but it allows the identification of possible modifications (e.g. cathode geometry and ion optics geometry) that could reduce the gap between xenon and the selected alternative propellants.

1. INTRODUCTION

Nowadays, xenon is the most common propellant used for space applications because of its favourable physical and chemical properties. However, it is particularly expensive due to its limited availability and complex extraction process. Therefore, the search for a viable alternative is gaining importance to meet the need for a growing diversification of satellites, missions, and manoeuvres. This aspect has been boosted by the "New Space" revolution, which demands cheaper and simpler systems even at the cost of lower performance.

An initial assessment [1] was carried out through a comprehensive review of the published data on the usage of alternative propellants, such as other noble gases, iodine, and other more exotic propellants (i.e. Buckminsterfullerene and Adamantane), followed by a qualitative and quantitative analysis of the impact of the alternative propellants on the different parts of a GIE's systems and on performance. Based on these preliminary results, krypton and a mixture of Xe/Kr appear to be effective alternatives if all of the selected impacts are taken into consideration [2], [3], since only minimal variations to the existing propulsion systems are expected.

The objective of this paper is to further investigate the performance gap between xenon (as baseline) and the selected alternative propellants (i.e. krypton and a mixture of Xe/Kr). This investigation was primarily carried out through an experimental campaign with a small ring-cusp gridded ion engine, which was tested and characterised using the simulated beam extraction technique described by Brophy [4].

The paper is organised as follows. In Section 2, the experimental setup is described in detail. Section 3 presents and discusses the experimental characterization carried out in this activity. Finally, general conclusion and possible perspectives are summarized in Section 4.

2. EXPERIMENTAL SETUP

The experimental campaign, which allowed the evaluation and quantification of the impact of propellants alternative to xenon (i.e. krypton and Xe/Kr mixture), was performed using a small RCDC with an extraction grid diameter of 10 cm, which was designed and manufactured by Mars Space Ltd (MSL), based on their experience with the development of a larger ring-cusp discharge chamber (RCDC) [5], [6].

The discharge chamber's shape, and the number and position of the magnet rings are similar to other thrusters of this size present in the literature [7]. A schematic of the discharge chamber with the

position of the magnets is shown in Figure 1: two magnet rings are positioned along the straight part of the discharge chamber and one along the conical section.

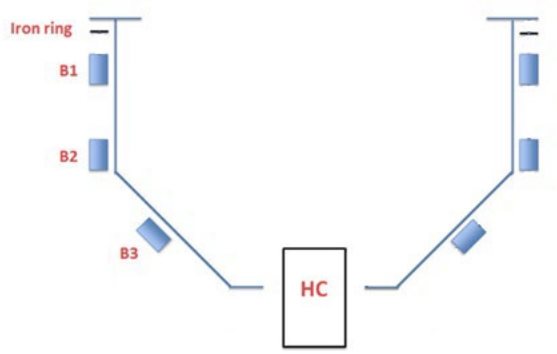

Figure 1 – Schematic of the discharge chamber (reference only).

Because of limitations on the pumping speed of the available vacuum chamber, the discharge chamber will run in a discharge-only mode without beam extraction using Brophy's method [4], so no neutralisation of the beam is required, and the injected mass flow rate is lower than that necessary for operation with beam extraction. In addition, the ingested gas from background pressure was calculated to be lower than 10% of the total mass flow rate injected through the discharge chamber during the experiment, which is a more than acceptable value.

2.1. Vacuum Chamber

The small RCDC was tested inside the MSL-VC1 vacuum chamber, shown in Figure 2. It consists of a stainless-steel L-shaped chamber, 0.52 m in diameter and 1.2 m long, which is equipped with the following pumping system:

Figure 2 – VC1 vacuum chamber in MSL propulsion laboratory.

- an Edwards xDS35i dry scroll pump for low vacuum with a pumping speed of 35 m^3/h was used to bring the chamber pressure down to $5x10^{-2}$ mbar and as a backing pump for the turbopump,
- an Edwards STP-iXA4506C turbo-molecular pump for high vacuum, which gives an effective xenon pumping speed of 3000 L/s and achieves a base pressure below $1x10^{-7}$ mbar.

The pressure inside the chamber was measured by a calibrated Kurt J. Lesker KJLC 354 Series Ion Gauge, with pre-configured correction factors for the gases used, which covers the high vacuum pressure range.

2.2. Fluidic Setup

A Fluid Ground Support Equipment (FGSE) was designed to supply the gas inlets (i.e. main and the hollow cathode) of the discharge chamber with xenon and krypton at the desired flow rate, as shown in Figure 3.

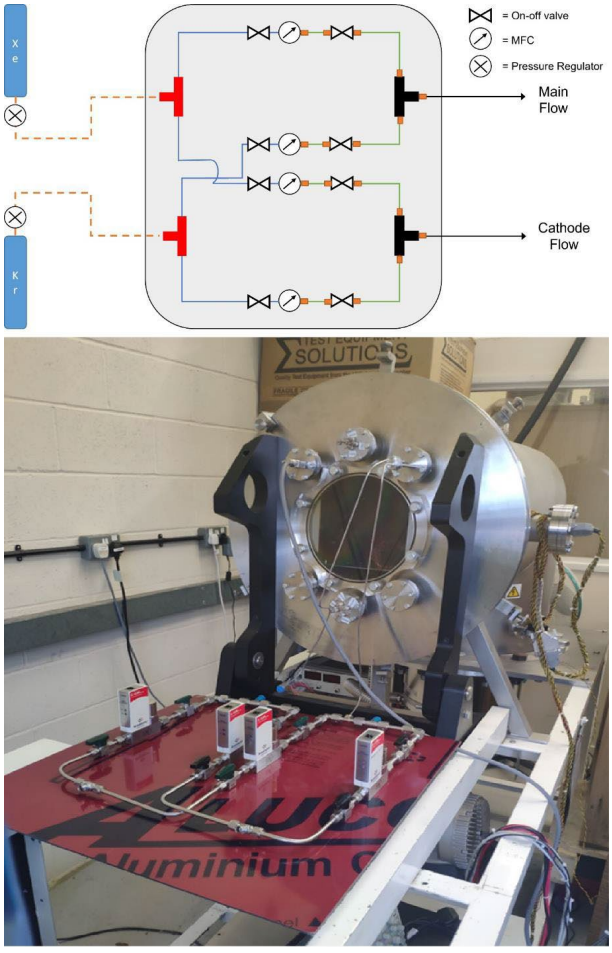

Figure 3 – Fluidic setup.

Xenon and krypton were supplied from two independent cylinders equipped with their own pressure regulator, which maintains a constant upstream (i.e. up to the mass flow controllers, MFCs) pressure of 2.5 bar during the test. Two pairs of Bronkhorst factory calibrated MFCs were used to regulate the flow rate to the cathode and discharge

chamber independently within the following flow rate ranges:

- for the cathode line: two MFCs with a range of 0-10 sccm and calibrated for Xe and Kr
- for the main line: two MFCs with a range of 0-5 sccm and calibrated for Xe and Kr.

Furthermore, this setup was designed to allow the testing of a mixture of xenon and krypton at the desired mixture ratio of 1:4.

Moreover, all airside FGSE piping is 1/4" stainless steel with Swagelok connectors used on the high-pressure joints and with Swagelok VCR seals used on the low-pressure joints to minimise the risk of air leaks. Finally, a series of on/off manual valves are in place to enable the isolation of various parts of the FGSE.

2.3. Electrical Setup

MSL's Electric Ground Support Equipment (EGSE) was used for the test campaign, and it consists of a dedicated rack comprising of:

- several power supplies rated and interconnected to supply the small RCDC with the power it needs to operate,
- a digital multiplexer monitoring currents, voltages and temperatures (via thermocouples) used to measure the status of the thruster,
- a dedicated hardware protection system operating independently to disable the power supplies with a hard shutdown to protect both the hardware and the personnel.

The schematic of the electrical setup is presented in Figure 4 and it is similar to the one used by MSL in previous experiments [5], which is based on the one used by Brophy [4]. This setup allows the operation of the discharge chamber without beam extraction and estimates the expected performance with beam extraction by measuring the ion current collected at the grids.

The main characteristics of this setup are:

- The discharge chamber body is electrically isolated from the vacuum chamber, which is connected to the facility ground.
- The cathode heater is operated when required using the keeper supply, which will be switched to the heater line via a dedicated relay.
- The screen and accel grids can be biased at various potentials using a dedicated grid supply to repel electrons while allowing the measurement of the collected ion current.
- The cathode (i.e. negative of the anode supply) is connected to an "engine bias" supply which allows biasing of the engine up to 20 V positive with respect to the ground in accordance with Brophy's method to avoid the escape of electrons from the discharge chamber volume. The residual ion beam leaving the discharge chamber is expected to be in the order of tens of mA.

In Figure 4, all voltages and currents are recorded directly and independently from the relative power supplies via the multiplexer. In addition, two differential probes whose signal is acquired by an oscilloscope are used to monitor the voltage and the associated peak-to-peak noise of the cathode keeper and the anode relative to the cathode.

Finally, all the discharge chamber control commands and data acquisition are done using a LabView program which communicates with the instrumentation (i.e. multiplexer, oscilloscope,

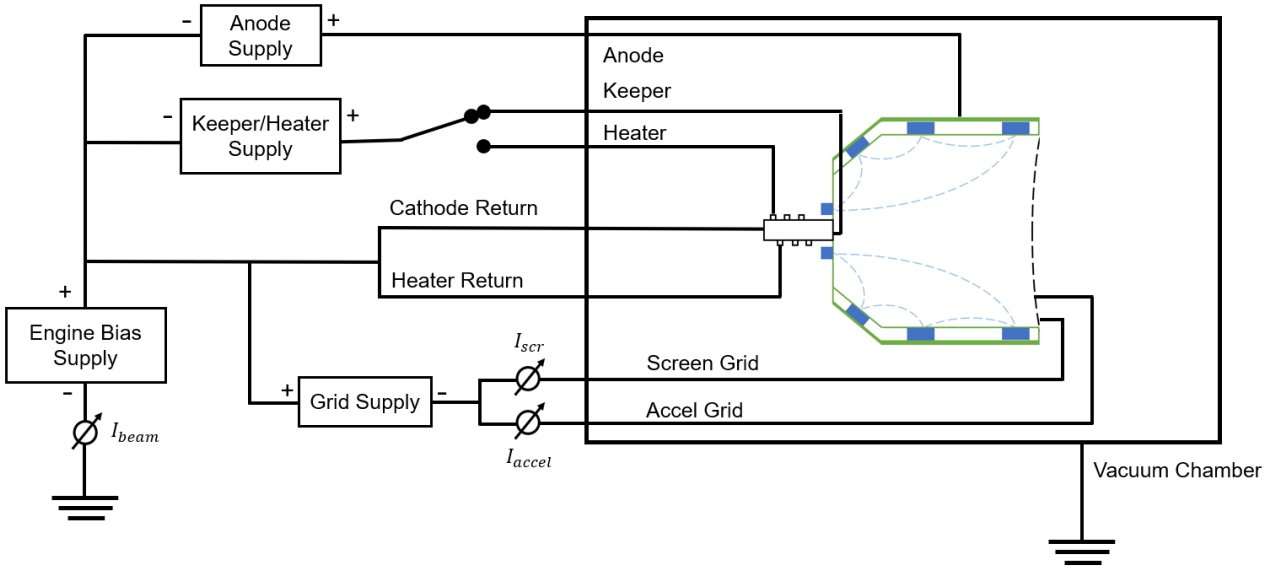

Figure 4 – EGSE setup (without beam extraction).

power supplies, and MFCs) using USB/RS232 connections. In addition, optocouplers are used to isolate the control system from electrical discharges caused by the test apparatus.

2.4. Test Overview

As mentioned above, the main objective of the test campaign was to conduct a performance characterisation of the small ring-cusp discharge chamber with xenon and the selected alternative propellants (i.e. krypton and the 1:4 Xe/Kr mixture) running the thruster in discharge-only mode and using Brophy's technique to simulate the performance with beam extraction.

The characterisation of the thruster performance was carried out as follows:

- firstly, a baseline performance characterisation was obtained by running the discharge chamber with xenon at known stable operating conditions (from previous tests)
- secondly, keeping the anode and keeper current fixed (equal to 4.5 A and 0 A, respectively), various operational points for the cathode flow rate were tested in order to identify a few points with stable operating conditions (e.g. stable voltage discharge) for the other two propellants (three for Kr, and two for the 1:4 Xe/Kr mixture)
- finally, for the selected cathode flow rates, the main flow rate was tuned in order to obtain the selected propellant utilisation efficiencies (between 0.6 and 0.85, where possible, with increments of 0.05).

The resulting configuration set points were:

- Discharge current = 4.5 A
- Beam voltage: 1200 V
- Cathode flow rates:
  - Xenon = 1.2 sccm
  - Krypton = 1.5, 1.6 & 1.9 sccm
  - 1:4 Xe/Kr mixture = 1.5 & 1.625 total sccm
- Propellant utilisation efficiency = from 0.6 to 0.85 (when possible, because of limitations on the minimum main flow rate).

Furthermore, it is worth highlighting that the small RCDC and the relative hollow cathode used for the testing are in development to run mainly with xenon, and that the tests with alternative propellants were carried out using the same thruster configuration (e.g. hollow cathode orifice, ion optics, magnetic fields) as with xenon.

3. PERFORMANCE RESULTS OF THE SMALL RCDC

Using Brophy's technique [4], in order to estimate the equivalent performance and operating conditions of a discharge chamber tested without beam extraction if the high voltage was applied to the grids, the following identities are used:

- Ion beam current [A]:

$$I_b = \sum_j I_{tot,j}\, T_{beam,j} \qquad \text{Eq. 1}$$

- Mass utilisation efficiency:

$$\eta_m = \sum_j \frac{I_{b,j}}{e\frac{\dot{m}_{dc,j}}{M,j} + I_{b,j}\left(1-\frac{T_{dc}}{T_{beam,j}}\right)} \qquad \text{Eq. 2}$$

- Total mass flow rate [sccm]:

$$\dot{m}_p = \sum_j \frac{\dot{m}_{dc,j}}{1-\eta_{m,j}\left(1-\frac{T_{dc}}{T_{beam,j}}\right)} \qquad \text{Eq. 3}$$

- Discharge loss [W/A or eV/ion]:

$$\eta_d = \frac{I_d V_d}{I_b} = \frac{(\hat{I}_d - I_b)\hat{V}_d}{I_b} \qquad \text{Eq. 4}$$

where the symbol $\widehat{\ }$ and the subscript dc designate the case without beam extraction. Eqs. 1-4 are expanded to include the case when a mixture of gases is used and the subscript j represents the j-th ion species.

In Eq. 1, the ion optics transparency, T_{beam}, was calculated using an ion optics code (i.e. FFX) and the results are shown in Figure 5 as a function of the total current reaching the grids' plane.

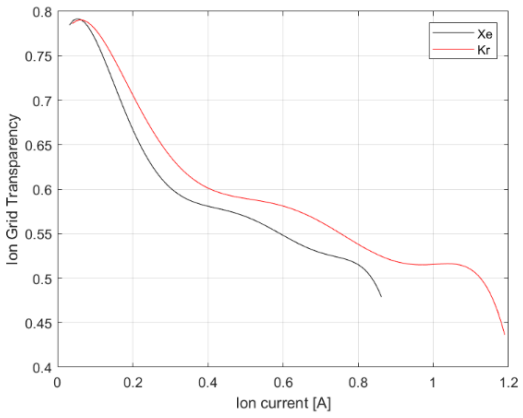

Figure 5 – Ion optics transparency for xenon and krypton.

3.1. Discharge Loss Trends

A typical way to characterise the discharge chamber performance of an ion thruster is by plotting the discharge loss as a function of the propellant utilisation efficiency, the so-called performance

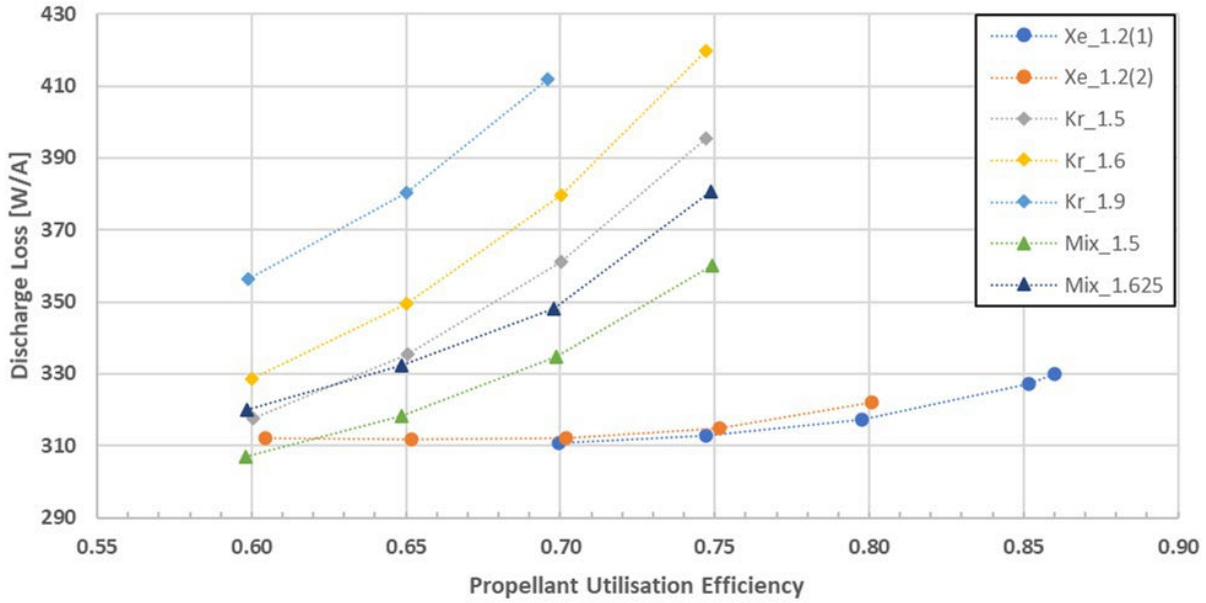

Figure 6 – Simulated discharge losses and their trends.

curve. However, it is worth highlighting that performance curves are normally taken at constant beam current and discharge voltage so that the efficiency of producing and delivering ions to the beam is not masked by changes in the discharge voltage or average plasma density at the grids. Figure 6 compares the simulated discharge losses (calculated using Eq. 4) for xenon, krypton and the mixture for a given propellant efficiency (calculated using Eq. 2). Since the characterisation has been carried out at a constant discharge current, the dotted lines in Figure 6 represent the trend curves in the discharge loss and not the performance curves.

The discharge losses when using krypton are higher than those obtained with xenon and the gap, small at lower efficiencies, increases substantially moving towards higher efficiencies. The difference in discharge losses can be mainly linked to the difference in discharge voltages (on average 4 V higher for krypton as shown in Section 3.3) and a possible lack of optimisation for krypton (e.g. related to the ion optics and the cathode geometries).

The performance with the mixture is expected to be between that of pure xenon and that of pure krypton: at lower efficiencies, the discharge losses for the mixture tend to converge with those of xenon and krypton, but the presence of xenon seems to mitigate the losses obtained with pure krypton at higher utilisation efficiencies. This result is very promising, and it requires further investigation to confirm it.

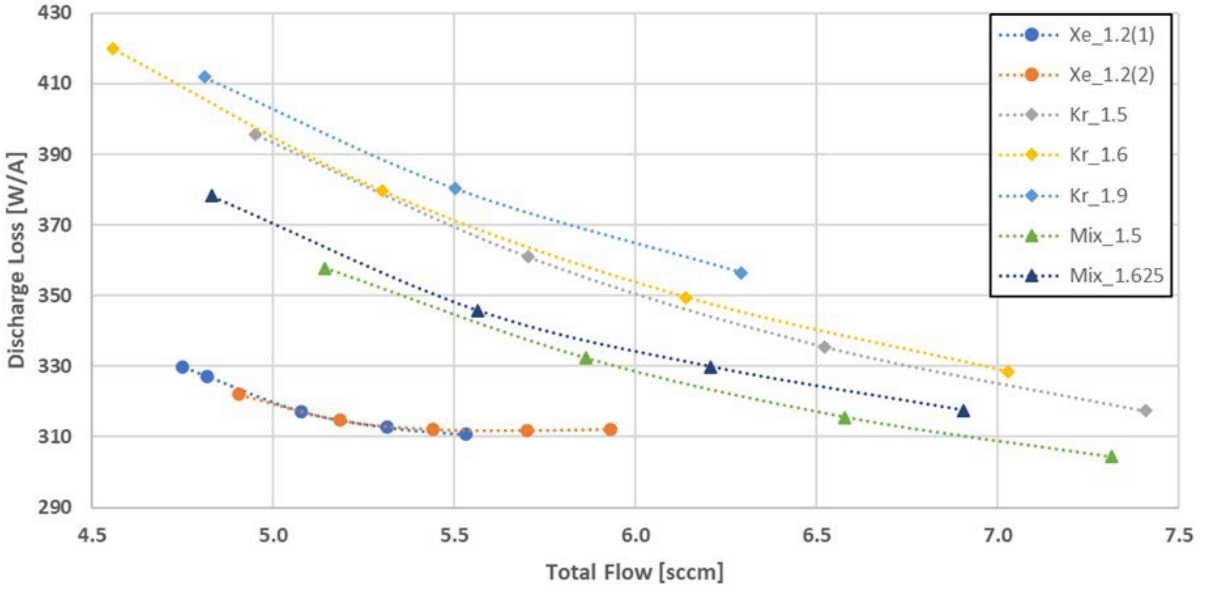

Figure 7 – Discharge loss as a function of total flow rate in sccm.

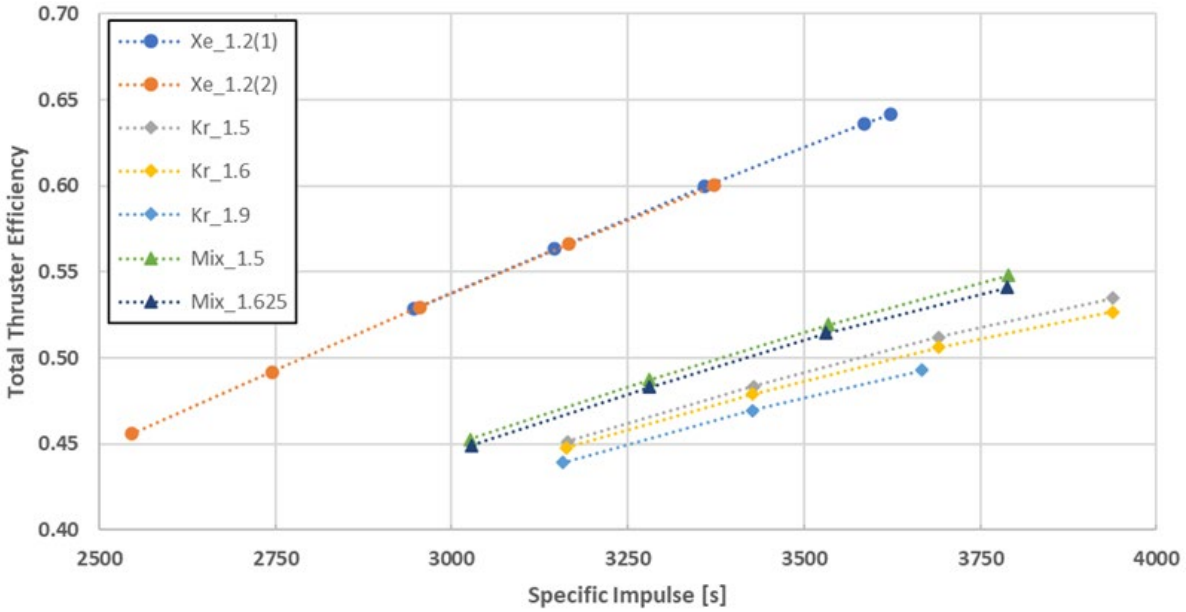

Figure 8 – Total thruster efficiency as a function of specific impulse.

Finally, Figure 7 shows the discharge loss as a function of the total volumetric flow rate into the thruster in sccm (calculated using Eq. 3). It can be observed that there is a trend with the discharge loss decreasing when increasing the propellant mass flow rate as expected, where the use of alternative propellants introduces a clear penalty in terms of W/A for equivalent flow rates, and the difference is in the range of 20-40 W/A for the mixture and 40-80 W/A for krypton.

3.2. Specific Impulse Trends

Although a performance gap exists between xenon and the alternative propellants under investigation, Figure 8 shows one of the benefits of using krypton and the mixture: at similar thruster efficiencies, the specific impulse is higher than with xenon, as expected from the definition of specific impulse and its dependence on the square root of the propellant atomic mass. The values for the specific impulse and total thruster efficiency are reported below, including the case for mixtures:

$$I_{sp} = \sum_j \frac{T_j}{\dot{m}_{p,j} g_0} = 1.417x10^3 \gamma \sqrt{V_b} \sum_j \eta_{m,j} \frac{1}{\sqrt{M_{a,j}}} \quad \text{Eq. 5}$$

$$\eta_T = \gamma^2 \eta_e \eta_m \quad \text{Eq. 6}$$

However, the overall thruster efficiency is approximately 10% lower with alternative propellants than that with xenon at a given specific impulse. Interestingly, the results with the mixture are much closer to those obtained with pure krypton compared for example to the trends seen in Figure 6, where the mixture was almost halfway between pure xenon and pure krypton.

Furthermore, it has been demonstrated that it is possible to increase the maximum obtainable specific impulse with krypton even further by using optimised ion optics (e.g. with lower neutral transparency) and higher beam voltages [8].

3.3. Voltage Trends

The plot of discharge voltage as a function of propellant utilisation efficiency is shown in Figure 9. As expected, higher discharge voltages are required for krypton compared to those for xenon, and this behaviour can be associated mainly with krypton's higher ionisation energy compared to xenon (14 eV vs 12.1 eV). However, the discharge voltage with krypton has a smaller gradient when increasing the efficiency compared to the values with xenon, which show a slightly steeper increment. This difference in discharge voltages between krypton and xenon partially explains the difference in discharge losses, as seen in Section 3.1, which are directly proportional to the discharge voltage. The figure also shows that the values of the discharge voltage for the mixture are between that of pure xenon and that of pure krypton, showing a similar behaviour to that of pure krypton.

The higher discharge voltages obtained for the alternative propellants are likely to have an impact on the lifetime of both the internal walls of the discharge chamber at anode potential and of the ion optics (i.e. the screen grid, in particular), due to the higher energy of the ions and electrons impacting these surfaces. In fact, krypton has higher sputter yields compared to xenon at the same impact energy with materials typically used for ion optics (e.g. it is roughly double with graphite grids [9]).

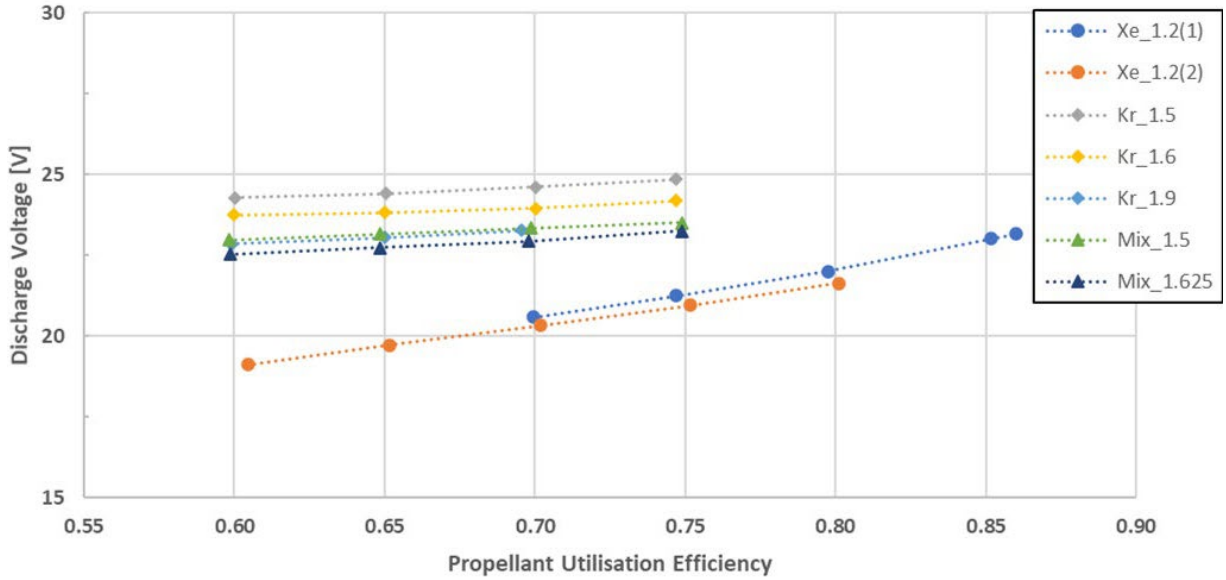

Figure 9 – Discharge voltage as a function of propellant utilisation efficiency.

3.4. Power Trends

The total thruster efficiency as a function of the total input power is shown in Figure 10. The total input power was calculated as follows:

$$P_{tot} = I_b V_b + I_d V_d + P_{other} \qquad \text{Eq. 7}$$

where $P_b = I_b V_b$ is the beam power, $P_d = I_d V_d$ is the discharge power and P_{other} represents the other power input to the thruster required to create the thrust beam (e.g. cathode heater and keeper power, neutraliser power, etc.). In this case, the total power can be considered to be almost directly proportional to the beam current I_b, since the beam voltage and the discharge current are kept constant, the discharge voltage does not change much for the different propellants (as seen in the previous subsection), and P_{other} has been assumed to be zero for these calculations (in fact, the cathode heater was turned off during the operations, the cathode keeper was floating, and the neutraliser was not present since there was no extracted beam to neutralise).

The results obtained for the various propellants are conflicting: the thruster efficiency increases for xenon when the total current I_{tot} increases, but the opposite is true for the alternative propellants under consideration. The reasons for this behaviour are not clear, and the assumption is that it is related to the balance of the energy loss mechanisms within the discharge chamber, such as excitation, ionisation, and ion and electron losses. Furthermore, the inconsistent nature of this phenomenon has been identified in a similar test run at MSL's facilities

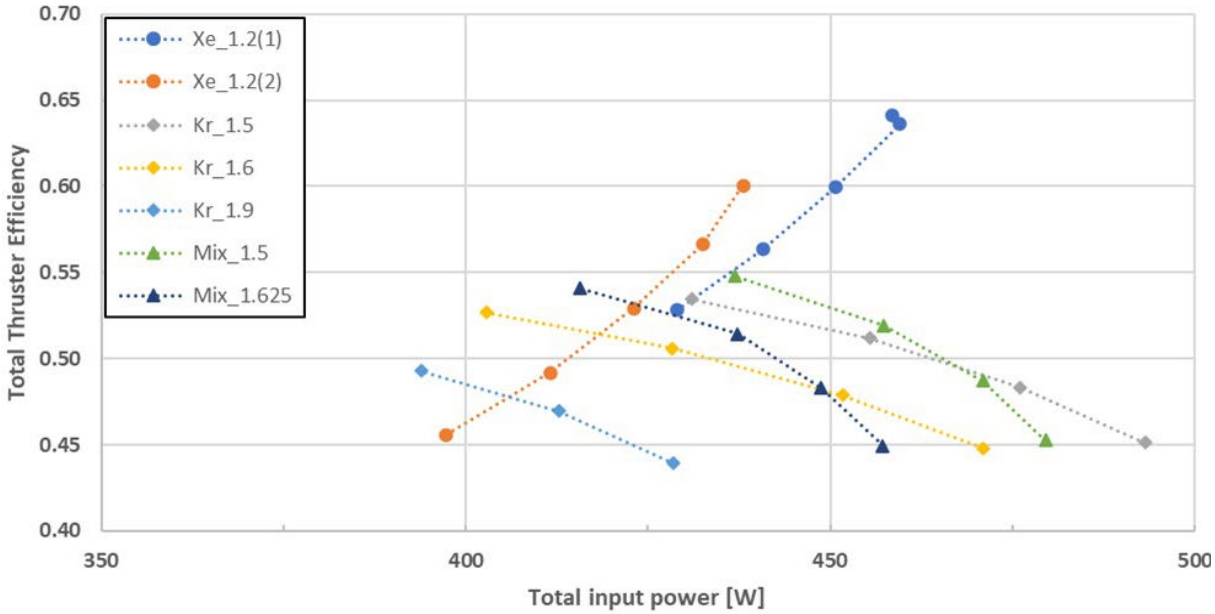

Figure 10 – Total thruster efficiency as a function of total input power.

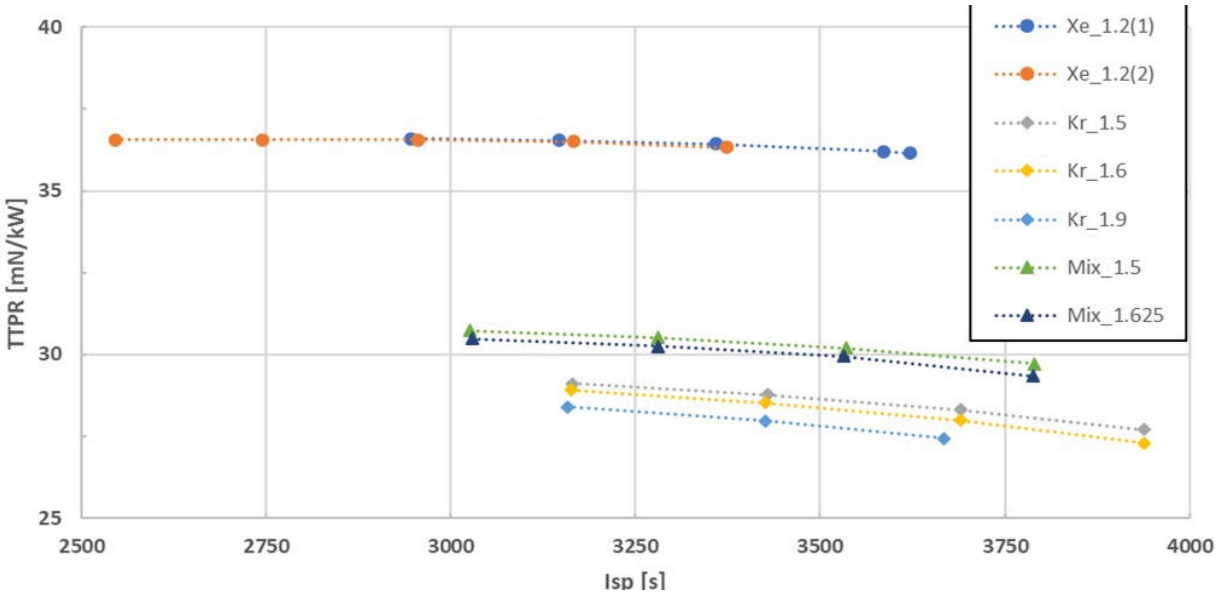

Figure 11 – Thrust-to-Power ratio as a function of specific impulse.

with a bigger RCDC [10] using xenon as propellant: in that specific case, the total thruster efficiency increases or decreases with the total input power depending on the discharge power levels, and, in particular, they both increase at the highest power level (i.e. discharge current of 28 A) but not and the lower power levels (i.e. medium and low power levels with a discharge current of 20 A and 15 A, respectively).

This behaviour was highlighted during the data analysis phase, and it was not possible to verify it with further tests, but it will need to be considered during any future testing campaign.

Figure 11 shows the thrust-to-power ratio (TTPR) as a function of the specific impulse for the three propellants. The separation between xenon and the considered alternative propellants is quite evident: xenon is the best choice when the thrust is the most important parameter for the mission, but, if specific impulse is more important during the mission design phase, krypton and the mixture have an advantage if a penalty of about 20% in TTPR is acceptable (i.e. longer missions but with higher specific impulse).

4. CONCLUSIONS

A small ring-cusp GIE, in development to be used with xenon, has been tested with xenon and two alternative propellants (krypton and a 1:4 Xe/Kr mixture) to identify the baseline performance gap between the different propellants. This represents the worst-case scenario for alternative propellants, but it allows the identification of possible modifications (e.g. cathode geometry and ion optics geometry) that could reduce the gap between xenon and the selected alternative propellants, making them a more attractive proposal for future use.

5. ACKNOWLEDGMENTS

The authors would like to thank the University of Southampton, the Tony Davies High Voltage Lab (TDHVL) and Mars Space Ltd for the support. This research has been funded by the European Commission in the scope of the GIESEPP project, within the frame of the H2020 Research program - COMPET-3-2016-a SRC - In-Space Electrical Propulsion and Station Keeping, Incremental Line - Gridded Ion Engines of the European Union (Research and Innovation contract No 730002).

6. REFERENCES

[1] N. Fazio, S. B. Gabriel, and I. O. Golosnoy, “Alternative Propellants for Gridded Ion Engines,” in *6th Space Propulsion Conference*, 2018, pp. 1–8.

[2] N. Fazio, S. B. Gabriel, I. O. Golosnoy, and B. Wollenhaupt, “Mission Cost for Gridded Ion Engines using Alternative Propellants,” in *36th International Electric Propulsion Conference*, 2019, pp. 1–21. [Online]. Available: https://eprints.soton.ac.uk/434549/

[3] N. Fazio, I. O. Golosnoy, and S. B. Gabriel, “Discharge Performance Analysis of different types of Gridded Ion Engines using Alternative Propellants,” in *37th International Electric Propulsion Conference*, 2022, pp. 1–14.

[4] J. R. Brophy, “Simulated Ion Thruster Operation without Beam Extraction,” in *21st AIAA/DGLR/JSASS International Electric Propulsion Conference*, Jul. 1990. doi:

10.2514/6.1990-2655.

[5] F. Cannat, F. Guarducci, S. Ciaralli, M. Coletti, and S. B. Gabriel, “Design and Optimization of a Ring Cusp Thruster with Simulated Beam Extraction,” in *35th International Electric Propulsion Conference*, 2017.

[6] F. Cannat, F. Guarducci, S. Ciaralli, and S. B. Gabriel, “Development of a 30-cm Ring Cusp Discharge Chamber - Design and Performance Characterization with Simulated Ion Beam Extraction,” in *6th Space Propulsion Conference*, 2018.

[7] R. E. Wirz and F. E. C. Culick, “Discharge Plasma Processes of Ring-Cusp Ion Thrusters,” California Institute of Technology, Pasadena, California, USA, 2005. [Online]. Available: http://resolver.caltech.edu/CaltechETD:etd-05232005-162628

[8] M. J. Patterson and J. G. J. Williams, “Krypton Ion Thruster Performance,” in *28th AIAA/SAE/ASME/ASEE Joint Propulsion Conference and Exhibit*, 1992. doi: 10.2514/6.1992-3144.

[9] E. Oyarzabal, R. P. Doerner, M. Shimada, and G. R. Tynan, “Carbon Atom and Cluster Sputtering under Low-Energy Noble Gas Plasma Bombardment,” *J. Appl. Phys.*, vol. 104, no. 4, Aug. 2008, doi: 10.1063/1.2968549.

[10] F. Bosi, F. Cannat, F. Guarducci, and S. B. Gabriel, “Experimental Characterization of a Ring-Cusp Discharge Chamber with Xenon and Krypton,” in *37th International Electric Propulsion Conference*, 2022, pp. 1–13.